

N66 35318

(ACCESSION NUMBER)

29

(PAGES)

TMX-56962

(NASA CR OR TMX OR AD NUMBER)

(THRU)

1

(CODE)

30

(CATEGORY)

THE SEMICONVECTIVE ZONE IN VERY MASSIVE STARS

~~Richard Stethers~~

Institute for Space Studies
Goddard Space Flight Center, NASA
New York, N.Y.

GPO PRICE \$ _____

CFSTI PRICE(S) \$ _____


Hard copy (HC) 2.00

Microfiche (MF) .50

ABSTRACT

353/8

Models are constructed for very massive stars in the range $45 M_{\odot}$ to $1000 M_{\odot}$ during hydrogen burning, in order to examine the role of convective instability. The semi-convective zone shows a maximum growth (in mass fraction) at about $60 M_{\odot}$, with a chosen initial hydrogen abundance of $X = 0.70$. Sixty M_{\odot} is also the maximum mass found by Schwarzschild and Härm to be stable against radial pulsations, for nearly the same chemical composition. Radiation pressure has a critical destabilizing influence here. In the limit of the highest masses, the semiconvective zone disappears toward the surface, but the star still evolves inhomogeneously. It is shown that asymptotic limits at hydrogen exhaustion exist for the mass fraction of the convective core, the mean hydrogen content, and the hydrogen-burning lifetime.



I. INTRODUCTION

Theoretical understanding of very massive stars depends critically on a knowledge of the mechanism and extent of internal mixing. This mixing may be due to rotation or convective instability. In the present paper, models are constructed for stars which are strongly unstable to convection outside the normal convective core, but which are non-rotating. The assumption of convective neutrality in the unstable part of the envelope permits calculation of the extent of mixing phenomenologically, without reference to the details of convection theory. A description of the so-called semiconvective zone which is formed has been given in Paper I (Stothers 1963). The present paper investigates the extent of the semiconvective zone and convective core as a function of stellar mass and evolution during hydrogen burning.

II. ASSUMPTIONS

The general structure of a very massive star has been described in Paper I. We adopt the same assumptions, defi-

nititions, and notations as before. The age-zero chemical composition is again taken to be

$$X_0 = 0.70, Y_0 = 0.27, Z_0 = 0.03, \mu_{00} = 2/3.$$

The opacity is assumed to be due only to electron scattering, $\kappa = 0.19(1 + X)$, and the equation of state is represented by the sum of the perfect-gas and radiation pressure. The parameters in the nuclear-energy generation formula are adequately given by $\nu = 14$ and $\log \epsilon_0 = -99.0$, for all the present models. For simplicity, we assume the full equilibrium abundance of oxygen. The approximation in the nuclear rate will affect only the dimensional structure of the models, and will therefore have no bearing on the distribution of chemical composition, zonal boundaries, or time scale of evolution, which comprise the main subject of this paper. These non-dimensional quantities should be especially well determined in our models since comparison with Los Alamos opacities (Ezer and Cameron 1965) indicates that the simple electron-scattering opacity assumed here will be an excellent approximation throughout the star practically to the stellar surface, for such high masses as we are considering.

Allen's (1963) values of solar luminosity and radius were used as normalizing quantities, whereas, in Paper I,

Chandrasekhar's (1939) values were used. A subscript f refers to the boundary of the convective core at the evolutionary stage when hydrogen is just exhausted in the core.

III. MODELS OF VERY MASSIVE STARS

The main characteristics of models for six very massive stars during hydrogen burning are presented in Table 1. The models were calculated automatically by an IBM 7094 computer, with the semiconvective zone taken explicitly into account, as described in an earlier paper (Stothers 1966). This method of treatment of the semiconvective zone, while precise, gives results nearly identical with those calculated on the basis of the zone assumed radiative (Sakashita and Hayashi 1961; Stothers 1963, 1965). However, the latter method does not give correct results when the zone exceeds an extent of $\Delta q = 0.2$ (Stothers 1966).

a) Homogeneous Models

Were the models to form a homologous sequence, we should have exactly that $L \sim M^3$ and $q_4 = \text{constant}$. However, the models are far from homologous because of the wide variation in radiation pressure. On the basis of the standard

model, Eddington (1926) showed that the relative radiation pressure, $1-\beta$, increases with total stellar mass (through the well-known quartic equation). Since a large radiation pressure promotes convective instability by lowering the adiabatic temperature gradient, the mass fraction contained within the convective core will also be larger at the higher masses (Fig. 1). This may be seen precisely from the condition defining the convective core boundary, viz. equating the radiative and adiabatic effective polytropic indices at q_4 and introducing the approximate mass-luminosity relation $L \sim M^3$. Thus a sufficiently large mass becomes completely convective. The photon flux escaping from the surface is then determined entirely by the radiative surface condition,

$$\kappa_e L/M = 4\pi c G (1 - \beta_0). \quad (2)$$

In this case, the mass-luminosity relation approaches $L \sim M$.

b) Inhomogeneous Models

For the lower-mass stars in which radiation pressure is not dominant, the luminosity increases during evolution in accordance with the trend indicated by the homologous relation $L \sim M^4$. However, as $1 - \beta_0$ approaches unity in the higher masses, the luminosity remains constant if the star does not evolve fully mixed (such mixing would reduce X_e

and hence κ_e in eq. [2].

It may be simply shown that stars of even the highest mass must evolve inhomogeneously. Consider the core boundary for a star in which $\beta \approx 0$ throughout. Equating the radiative and adiabatic effective polytropic indices, we can obtain that $q_4 = \kappa_4/\kappa_e = (1 + X_4)/(1 + X_e)$. When hydrogen has been exhausted in the convective core, the core boundary must have shrunk to a mass fraction $q_f = (1 + X_e)^{-1}$. This implies a gradient of chemical composition left behind and sets an upper limit on the composition exponent, λ , in the intermediate zone. Hence the amount of hydrogen depletion is fixed for very massive stars. The minimum mean hydrogen content remaining after hydrogen burning will be $\bar{X} \approx X_e^2/2(1 + X_e)$.

Thus any star composed initially of pure hydrogen has a final $q_f \leq 0.50$ and $\bar{X} \geq 0.25$. For our chosen initial composition, the limiting values are $q_f \leq 0.59$ and $\bar{X} \geq 0.14$. Figure 1 shows the asymptotic approach of the core boundary toward a limiting value (slightly in excess of q_f since $X_c = 0.05$ in the figure) as the stellar mass is increased.

Sakashita, Ôno, and Hayashi (1959) have shown that semi-convective mixing cannot extend to the convective core: the steeper gradient of mean molecular weight in the deeper layers of the envelope inhibits the convective motions.

Thus the envelope can be only partially mixed. The unstable intermediate zone grows, however, as the luminosity increases during evolution. This results from the proportionate increase in relative radiation pressure (eq. [2]), which has a destabilizing influence on the gas.

The semiconvective zone has a maximum growth in stars with a critical mass near $60 M_{\odot}$ (Fig. 1). Stars of smaller mass feel strongly the destabilizing effect of increased radiation pressure as the mass is increased. However, above $60 M_{\odot}$, further increase of radiation pressure does not lower the adiabatic temperature gradient significantly (since n approaches 3 asymptotically). Moreover, the luminosity brightens very little during evolution of the more massive stars, causing near constancy of the conditions in the outer envelope. In fact, during evolution, the outward growth of the semiconvective zone is seriously limited since it is formed ab initio close to the stellar surface, and its inward growth is inhibited by the much steeper gradient of mean molecular weight occurring in the radiative intermediate zone of the more massive stars.

The increase of λ with stellar mass, however, masks the actual increasing extent of the radiative zone. The growing importance of this zone is due to the smaller amount

of semiconvection as q_0 approaches the surface for higher masses, and to the asymptotic limit to the increase of the convective core. Hence the gradient of hydrogen abundance with respect to mass fraction becomes gentler as the stellar mass is increased, reaching, like λ , an asymptotic limit (Fig 2).

The time scale of evolution of very massive stars is on the order of a million years. It does not change very much with increasing mass, because, although the luminosity is increasingly brighter, a larger fraction of the initial hydrogen content gets consumed. The time scale is given by

$$\tau = \int_{\bar{X}}^{X_e} (EM/L) d\bar{X}, \quad (3)$$

where $E = 6.0 \times 10^{18}$ gm/erg. Since, in the limit of extremely massive stars, \bar{X} at core hydrogen exhaustion approaches a constant value and $L \sim M$, it is clear that τ has a lower bound, viz.

$$\tau = \frac{E}{8\pi cG} \frac{x_e X_e (2 + X_e)}{1 + X_e}. \quad (4)$$

For an initial composition of pure hydrogen, $\tau = 2.16$ million years, and for our chosen initial composition,

$\tau = 1.36$ million years.

The evolutionary tracks of our models on the H-R diagram are shown in Figure 3. The locus of points representing models at the same evolutionary stage tends to curve over toward cooler effective temperatures at the highest masses, for the following reason. Let $L \sim M^\alpha$. Then since $R \sim M$, we have that $T_e \sim M^{(\alpha-2)/4}$ from the black-body surface relation. In the limit of very low masses, $\alpha = 3$ and so $T_e \sim M^{1/4}$; the effective temperature increases with mass (and luminosity). In the limit of very high masses, $\alpha = 1$ and so $T_e \sim M^{-1/4}$; then the effective temperature decreases with increasing mass.

IV. FINAL REMARKS

Schwarzschild and Härm (1958), among others, have also integrated sequences of stellar models for very massive stars during hydrogen burning. These earlier results, based on treatments of the unstable intermediate zone which were not entirely self-consistent, are nevertheless very similar to ours because of the insensitive dependence of the stellar structure on the composition modifications (Hoyle 1960; Paper I).

We therefore have confidence in some previous conclusions reached by these workers. In particular, Schwarzschild and Härm (1959) performed a stability analysis of their models of massive stars and found a maximum mass of $60 M_{\odot}$ which would be stable against radial pulsations. In an earlier paper (Stothers 1965), it was shown that at least the pulsational eigenfrequencies would be unaffected for various treatments of the semiconvective zone in such stars. We therefore suppose that the pulsational growth rates will also not be largely affected. In view of the violence of the calculated instability above $65 M_{\odot}$, it would seem that the critical mass must in any case be fairly well determined.

From the present work, $60 M_{\odot}$ is close to the mass at which the semiconvective zone has its greatest extent. The coincidence is not fortuitous since, as we have seen, the effect of radiation pressure on the convective instability increases rapidly up to $60 M_{\odot}$, whereafter it increases more slowly, asymptotically reaching a limit. Radiation pressure has a similar effect on the pulsational instability (likewise enhanced as n approaches 3).

Boury (1963) obtained a maximum stable mass of $280 M_{\odot}$ for stars composed of pure hydrogen. Since the models of Schwarzschild and Härm had a hydrogen content of 0.75, we might expect that the critical mass for pulsational sta-

bility in our models would be slightly less than $60 M_{\odot}$.

This work was supported by an NAS - NRC postdoctoral research associateship under the National Aeronautics and Space Administration. It is a pleasure to thank Dr. Robert Jastrow for his hospitality at the Institute for Space Studies.

REFERENCES

- Allen, C.W. 1963, Astrophysical Quantities (London: Athlone Press).
- Boury, A. 1963, Ann. d'Ap., 26, 354.
- Chandrasekhar, S. 1939, An Introduction to the Study of Stellar Structure (Chicago: University of Chicago Press).
- Eddington, A. S. 1926, The Internal Constitution of the Stars (Cambridge: Cambridge University Press).
- Ezer, D., and Cameron, A.G.W. 1965, unpublished.
- Hoyle, F. 1960, M. N., 120, 22.
- Sakashita, S., and Hayashi, C. 1961, Prog. Theoret. Phys. (Kyoto), 26, 942.
- Sakashita, S., Ôno, Y., and Hayashi, C. 1959, Prog. Theoret. Phys. (Kyoto), 21, 315.
- Schwarzschild, M., and Härm, R. 1958, Ap. J., 128, 348.
- _____. 1959, ibid., 129, 637.
- Stothers, R. 1963, Ap. J., 138, 1074.
- _____. 1965, ibid., 141, 671.
- _____. 1966, ibid., 143, in press.

Evolutionary Models of Very Massive Stars during Hydrogen Burning

Model 0

Model 1

Model 2

i	0	1	2	3	4	1	2	3	4
U_i	1.33	1.11	1.17	1.18	1.43	0.760	0.890	0.912	1.56
V_i	5.18	5.16	4.84	4.86	4.67	5.06	4.07	4.18	4.04
$(n+1)_i$	3.46	3.52			3.56	3.64			3.73
$\log x_i$	-0.347	-0.365			-0.411	-0.410			-0.587
$\log q_i$	-0.157	-0.141	-0.158	-0.158	-0.198	-0.113	-0.174	-0.174	-0.295
$\log p_i$	0.483	0.513			0.735	0.589			1.345
$\log t_i$	-0.635	-0.615			-0.552	-0.572			-0.363
δ_i	0.775	0.747			0.729	0.685			0.622
X_i	0.700	0.700	0.699	0.693	0.582	0.700	0.679	0.648	0.307

$\log C$	-3.718	-3.660
λ		0.990
β_c	0.685	0.652
$\log T_c$	7.581	7.591
$\log \rho_c$	0.357	0.363
$\log (L/L_\odot)$	5.511	5.569
$\log (R/R_\odot)$	0.919	0.959
$\log T_e$	4.681	4.676
\bar{X}	0.700	0.622
τ (10 ⁶ years)	0.00	0.98

TABLE 1 -- Continued

M = 45 M_{\odot}

	Model 3				Model 4			
	1	2	3	4	1	2	3	4
i	0.621	0.749	0.779	1.58	0.544	0.654	0.689	1.57
U_i	5.01	3.68	3.83	3.89	4.97	3.44	3.63	3.87
V_i	3.69			3.80	3.72			3.83
$(n+1) i$	-0.434			-0.719	-0.452			-0.834
$\log x_i$	-0.099	-0.189	-0.189	-0.355	-0.092	-0.202	-0.202	-0.400
$\log q_i$	0.631			1.775	0.662			2.142
$\log p_i$	-0.551			-0.240	-0.537			-0.138
$\log t_i$	0.652			0.562	0.631			0.520
β_i	0.700	0.654	0.606	0.156	0.700	0.629	0.568	0.053
X_i								
$\log C$								
λ		-3.500				-3.470		
β_c		1.321				1.408		
$\log T_c$		0.515				0.479		
$\log \rho_c$		7.643				7.675		
$\log (L/L_{\odot})$		0.467				0.564		
$\log (R/R_{\odot})$		5.729				5.759		
$\log T_e$		1.167				1.235		
\bar{X}		4.612				4.585		
τ (106 years)		0.393				0.350		
		3.25				3.59		

TABLE 1 -- Continued

M = 60 M_{\odot}

	Model 0				Model 1				Model 2			
	0	1	2	3	4	1	2	3	4			
i	1.14	0.952	1.02	1.02	1.28	0.627	0.781	0.801	1.45			
U_i	5.89	5.83	5.46	5.48	5.17	5.66	4.46	4.57	4.34			
V_i	3.58	3.63			3.66	3.73			3.80			
$(n+1)i$	-0.316	-0.333			-0.383	-0.375			-0.568			
$\log x_i$	-0.120	-0.107			-0.161	-0.082			-0.258			
$\log q_i$	0.315	0.333			0.603	0.379			1.280			
$\log p_i$	-0.716	-0.700			-0.626	-0.667			-0.424			
$\log t_i$	0.720	0.690			0.669	0.621			0.556			
β_i	0.700	0.700			0.585	0.700			0.305			
X_i			0.698	0.693			0.674	0.643				
$\log C$	-3.851											
λ			-3.800				-3.700					
β_c	0.626		0.978				1.219					
$\log T_c$	7.597		0.592				0.505					
$\log p_c$	0.289		7.604				7.631					
$\log (L/L_{\odot})$	5.752		0.289				0.335					
$\log (R/R_{\odot})$	0.987		5.804				5.904					
$\log T_e$	4.708		1.026				1.147					
\bar{X}	0.700		4.701				4.665					
τ (10 ⁶ years)	0.00		0.616				0.443					
			0.82				2.24					

TABLE 1 -- Continued

M = 100 M_⊙

	Model 1				Model 2				
	0	1	2	3	4	1	2	3	4
i									
U _i	0.842	0.659	0.738	0.742	1.08	0.406	0.588	0.601	1.30
V _i	7.20	7.04	6.47	6.50	5.83	6.68	5.01	5.13	4.71
(n+1) i	3.74	3.78			3.81	3.85			3.90
log x _i	-0.270	-0.287			-0.361	-0.326			-0.575
log q _i	-0.072	-0.061	-0.075	-0.075	-0.123	-0.044	-0.095	-0.095	-0.222
log p _i	+0.003	-0.001			+0.464	-0.001			+1.297
log t _i	-0.870	-0.861			-0.738	-0.843			-0.505
β _i	0.616	0.576			0.549	0.501			0.434
X _i	0.700	0.700	0.697	0.690	0.557	0.700	0.662	0.633	0.266
log C	-4.129								
λ			-4.080					-4.000	
β _c	0.523		0.998					1.283	
log T _c	7.615		0.483					0.397	
log p _c	0.161		7.625					7.653	
log (L/L _⊙)	6.141		0.173					0.220	
log (R/R _⊙)	1.113		6.189					6.269	
log T _e	4.742		1.157					1.293	
\bar{X}	0.700		4.732					4.684	
τ (10 ⁶ years)	0.00		0.586					0.388	
			0.76					1.99	

TABLE 1 -- Continued

M = 100 M_⊙

	Model 3				Model 4			
	1	2	3	4	1	2	3	4
i	0.327	0.524	0.540	1.35	0.291	0.485	0.503	1.36
U _i	6.52	4.41	4.55	4.47	6.43	4.10	4.25	4.11
V _i	3.97			3.92	3.88			3.93
(n ₁₁) _i	-0.345			-0.714	-0.356			-0.810
log x _i	-0.038	-0.112	-0.112	-0.274	-0.035	-0.125	-0.125	-0.306
log q _i	+0.003			+1.786	+0.008			+2.119
log p _i	-0.835			-0.373	-0.831			-0.286
p _i	0.470			0.385	0.453			0.359
X _i	0.700	0.624	0.586	0.130	0.700	0.595	0.551	0.055
log C		-3.970					-3.955	
λ		1.422					1.502	
β _c		0.356					0.333	
log T _c		7.675					7.700	
log R _c		0.297					0.374	
log (L/L _⊙)		6.299					6.314	
log (R/R _⊙)		1.388					1.448	
log T _e		4.644					4.618	
\bar{X}		0.312					0.273	
τ (10 ⁶ years)		2.28					2.46	

TABLE 1 -- Continued

M = 200 M_{\odot}

	Model 3				Model 4			
	1	2	3	4	1	2	3	4
i	0.187	0.377	0.385	1.20	0.154	0.351	0.360	1.24
U _i	7.87	5.24	5.35	4.86	7.65	4.67	4.78	4.71
V _i	3.94			3.96	3.95			3.97
(n+1) i	-0.282			-0.683	-0.295			-0.829
log x _i	-0.017	-0.064	-0.064	-0.221	-0.014	-0.077	-0.077	-0.262
log q _i	-0.531			+1.684	-0.545			+2.211
log p _i	-1.096			-0.533	-1.096			-0.397
log t _i	0.343			0.284	0.321			0.255
β_i	0.700	0.634	0.610	0.152	0.700	0.598	0.570	0.049
X _i								
log C		-4.465					-4.450	
λ		1.459					1.540	
β_c		0.265					0.240	
log T _c		7.688					7.720	
log ρ_c		0.137					0.238	
log (L/L _c)		6.707					6.722	
log (R/R _c)		1.548					1.644	
log T _e		4.666					4.622	
\bar{X}		0.286					0.227	
τ (10 ⁶ years)		1.79					2.01	

TABLE 1 -- Continued

M = 400 M_⊙

	Model 3				Model 4			
i	1	2	3	4	1	2	3	4
U _i	0.103	0.269	0.272	1.11	0.081	0.261	0.264	1.16
V _i	9.31	5.95	6.02	5.10	8.95	5.10	5.17	4.89
(n+1) _i	3.97			3.98	3.98			3.99
log x _i	-0.232			-0.679	-0.246			-0.859
log q _i	-0.007	-0.038	-0.038	-0.193	-0.006	-0.051	-0.051	-0.239
log p _i	-1.041			+1.666	-1.071			+2.330
log t _i	-1.359			-0.677	-1.363			-0.507
β _i	0.243			0.205	0.223			0.181
X _i	0.700	0.645	0.631	0.161	0.700	0.607	0.592	0.046

log C	-5.000	-4.988
λ	1.458	1.563
β _c	0.194	0.172
log T _c	7.701	7.735
log ρ _c	-0.004	0.107
log (L/L _⊙)	7.075	7.087
log (R/R _⊙)	1.715	1.837
log T _e	4.675	4.617
\bar{X}	0.271	0.201
τ (10 ⁶ years)	1.52	1.75

TABLE 1 -- Continued

M = 1000 M_{\odot}

	Model 3				Model 4			
i	1	2	3	4	1	2	3	4
U_i	0.042	0.164	0.165	1.04	0.034	0.165	0.166	1.09
V_i	11.2	6.54	6.57	5.23	10.8	5.70	5.73	5.05
$(n+1)_i$	3.99			3.99	3.99			3.99
$\log x_i$	-0.187			-0.739	-0.197			-0.907
$\log q_i$	-0.002	-0.020	-0.020	-0.183	-0.002	-0.027	-0.027	-0.219
$\log p_i$	-1.685			+1.891	-1.724			+2.522
$\log t_i$	-1.705			-0.809	-1.714			-0.650
β_i	0.145			0.128	0.133			0.116
X_i	0.700	0.657	0.650	0.143	0.700	0.635	0.628	0.051

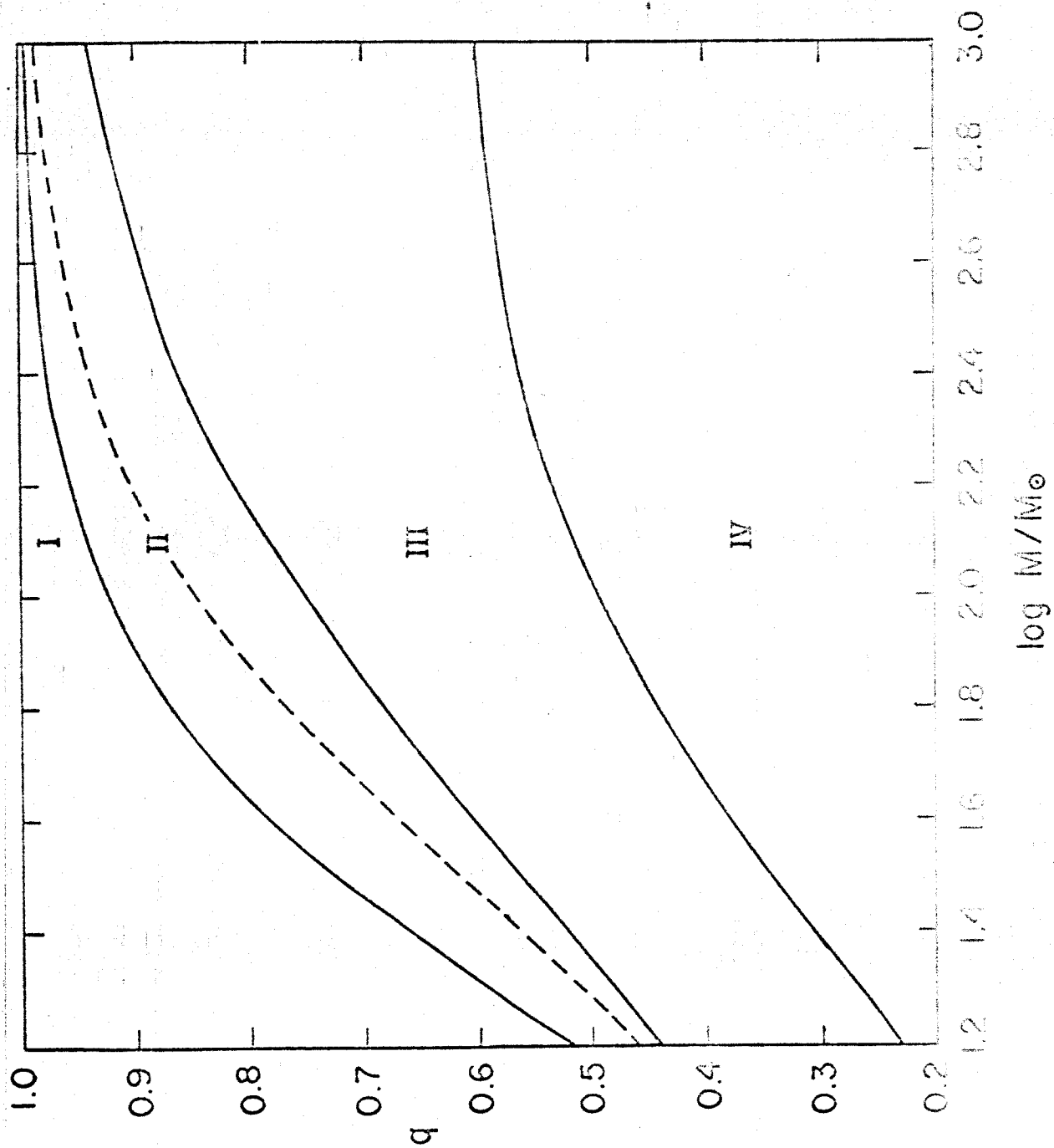
$\log C$	-5.740	-5.734
λ	1.497	1.581
β_c	0.124	0.112
$\log T_c$	7.721	7.749
$\log p_c$	-0.166	-0.074
$\log (L/L_{\odot})$	7.529	7.535
$\log (R/R_{\odot})$	1.977	2.096
$\log T_e$	4.657	4.599
\bar{X}	0.244	0.186
τ (10 ⁶ years)	1.38	1.54

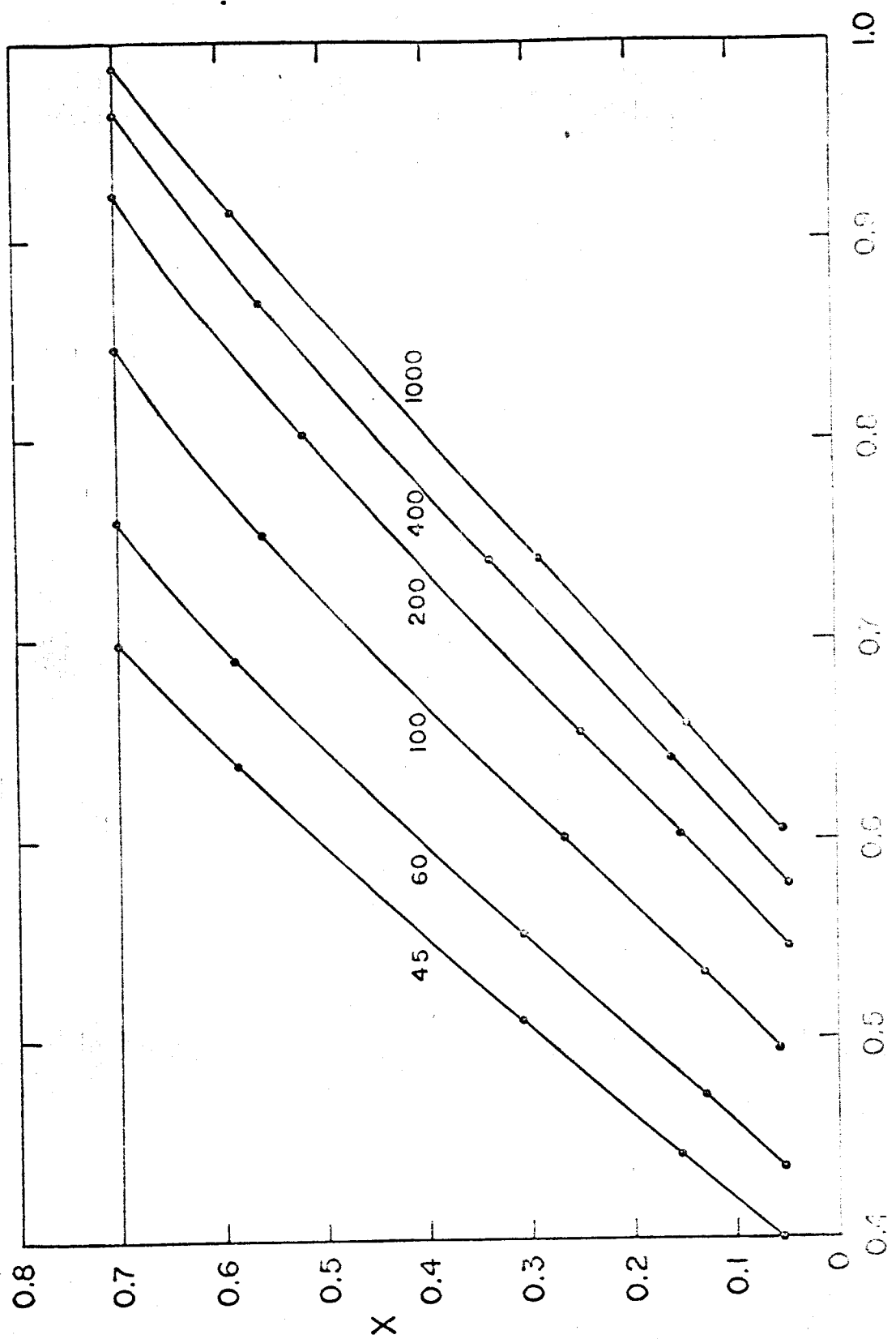
FIGURE LEGENDS

Fig. 1. — Mass fraction of the zonal interfaces in very massive stars when $X_c = 0.05$. The Roman numerals specify the outer radiative zone (I), semiconvective zone (II), radiative intermediate zone (III), and convective core (IV). The dashed curve refers to the mass fraction, q_0 , of the convective core on the initial main sequence.

Fig. 2. — Distribution of hydrogen in the radiative intermediate zone of very massive stars during hydrogen depletion. The composition modifications due to semiconvection are omitted. Dots represent the boundaries of the convective core for the various models. Numbers refer to the mass of the star in solar units.

Fig. 3. — Theoretical H-R diagram for very massive stars during hydrogen burning. Dashed curves are lines of constant time.





XERO
COPY

XERO
COPY

XERO
COPY

XERO

XERO

